# Monogenic Curvature Tensor as Image Model*

Gerald Sommer, Lennart Wietzke and Di Zang

gs@ks.informatik.uni-kiel.de
Department of Computer Science
Christian-Albrechts-University, Kiel, Germany

**Summary.** In this chapter, a new rotation-invariant generalization of the analytic signal will be presented to analyze intrinsic 1D and 2D local image structures. By combining differential geometry and Clifford analysis, the monogenic curvature tensor can be derived to perform a split of identity and to enable simultaneous estimation of local amplitude, phase, main orientation and angle of intersection in a monogenic scale-space framework.

## 1 Introduction

The processing and analysis of images and image sequences is a well established technology, although not fully satisfactory in some respect. Contemporary stated limitations have its reasons in the lack of a well founded and powerful theory of multi-dimensional signals. Because of the different topology of multi-dimensional signals in comparison to one-dimensional ones, serious consequences result with respect to formulation of a multi-dimensional signal theory. A signal theory should support the modeling of signal structures we are interested in and the operations we are applying to cope with certain tasks at hand. For both that signal theory should deliver useful representations. For instance, it is well known that the complex valued 1D Fourier transform enables a global view on the parity symmetry decomposition of a 1D function. Less known is the fact that this fails in case of the 2D Fourier transform because the possible symmetries are partially covered in the real and imaginary parts of the spectrum [42]. The central problem of modeling is the so-called representation problem. That is the problem of giving a certain concept a useful representation form. To cope with that problem in science and engineering, algebra as a mathematical language often delivers the right structure of representations. Also analysis and geometry as other resources of modeling are tightly related to algebra. Let us give two examples: First,

* This work was supported by DFG grant So 320/4-2 (GS,LW) and DFG Graduiertenkolleg No. 357 (DZ)

the holomorphic extension of a real valued 1D function to a complex one is a well-known method of complex analysis. But doing the same for a nD function requires another algebraic framework for analysis. The coupling of analysis with Clifford algebra establishes the Clifford analysis [7] as a useful approach to multi-dimensional functions. Second, the tight coupling of geometry with algebra is well-known since Felix Klein. Clifford algebra delivers algebraic structures for modeling any type of geometry which is particularly interesting in the case of multiple dimensions. Hence, we have to take advantage of the achievements in math for handling multi-dimensional functions. There are different interesting mathematical sources available which extend the representation of real valued multi-dimensional signals with the result that their structure becomes accessible. A well established concept is tensor algebra as generalization of vector algebra or matrix algebra [10]. Tensors are well-known as useful representations of geometry [11]. Clifford algebra or geometric algebra [22] is another concept, which only recently has been considered in engineering [40]. These algebras constitute other generalizations of the vector algebra, namely with respect to the representation of higher-order directed numbers, called multivectors. Both tensor algebras and geometric algebras deliver rich subspace structures in comparison to vector algebra. An advantage of geometric algebra over tensor algebra is its easier interpretation with respect to geometric concepts. Some entities contributing to the formulation of a problem can immediately represent geometry while possessing algebraic properties. Vice versa, the advantage of tensor algebra over geometric algebra is its easier numerical realization. Therefore, in practice it may be advantageous to transform expressions from geometric algebra to tensor algebra, see e.g. [41].

Very important in signal theory is the use of complex numbers. But according to our experience, complex numbers are only adequate to model one-dimensional signals. As already mentioned above, in the case of multi-dimensional signals, the algebraic framework has to be extended accordingly, see e.g. [42]. While Clifford algebra or geometric algebra supports a global view onto signal structures, Clifford analysis is useful for a local approach to signal analysis. The Hilbert transform takes over the role of the Fourier transform in the case of locally expanding a real valued one-dimensional function to a complex one. This corresponds to the holomorphic extension in complex analysis. In Clifford analysis we instead meet the Riesz transform which delivers a Clifford valued expansion of a real valued multi-dimensional function. The resulting representation is called a monogenic function. In both cases a real valued function will be completed by a harmonic conjugate which is in quadrature phase relation to the original real function. This most useful property will play a leading role throughout this chapter.

In this contribution, we are fusing the concepts of differential geometry for local image modeling in a tensor representation with the Clifford analysis concept of monogenic functions. This delivers a representation, called monogenic curvature tensor, which will enable local image analysis from one single

coherent mathematical point of view. The evaluation of the monogenic curvature tensor [48] delivers two curvature related signal representations which are specific for either intrinsically 1D or 2D structures. These signal representations are both generalizations of the well-known analytic signal [20]. From these Clifford valued signal representations local amplitude and local phase as local spectral representations as well as some geometric features can be computed. Because the monogenic curvature tensor is embedded in a monogenic scale-space [16], all features derived from it possess their own scale-space representation. Furthermore, the monogenic scale-space is the unifying framework for the scale related properties of all derived features.
In section 2, we will describe the required properties of the wanted signal model and the difficulties occurring in related work. In particular, we will give a short view on tensor based image analysis. In section 3, we will derive the monogenic curvature tensor and will present its evaluation. Finally, we will give a short summary and conclusion in section 4. Note that we will not give an introduction to geometric algebra or Clifford analysis. Instead, the reader is advised to have a look at [42] for a short introduction which is specific to the topic of that chapter. Other necessary hints are given at several places of this chapter.

## 2 Related Work

### 2.1 Key Point Detectors and Local Image Features

There are two basic tasks in low-level vision which are building a bottleneck in practise of image analysis, although plenty of work has been done over decades to overcome this situation. These tasks are the detection of points of interest and the analysis of their structure with respect to the neighborhood by a set of meaningful features. A detector is a local operator which has to fulfil two contradictory requirements: good recognition of the structure of interest and good localization accuracy. While the first one is located in a feature domain, the second one is located in spatial domain. In the case of LSI-operators and the frequency space as feature domain, the associated uncertainty principle is well-known [19]. Other problems with detectors are to model the structures of interest and to gain some invariance. While in 1D the number of different structures is quite limited, in 2D it is infinite. With respect to feature descriptors the problem is again to define a meaningful set of features and to gain certain invariance. Low-level image analysis is always model based. Because there is no satisfactory theory of multi-dimensional signal structures, the only chance is a comparison of different approaches out of a plenty of proposals, see e.g. [38] and [35]. The most prominent feature detector is SIFT [32]. Its model is very simple and the main bulk of work is shifted to classification in a high dimensional feature space. Other types of detectors are based on second order tensors (or matrices), e.g. the structure

tensor [17]. This detector in essence represents Gaussian smoothed partial derivatives of first order. Another kind of detector is based on the Hessian matrix, which is related to the curvature tensor of differential geometry [2], see e.g. [1]. These tensors are using derivatives of first and second order as elements. Therefore, they either represent gradient or curvature information. Because they are real valued, we propose in section 3 to unify the differential geometric point of view with the representation power of Clifford analysis.

### 2.2 Required Invariance

The image model we want to formulate should have some invariance properties. In general, image signals have no invariants in the strong sense of a quantity that does not change under a specified group of transformations. But there are some features which only slightly change by moderate changes of the conditions an image was recorded at. This is called weak invariance. We will use the term invariance instead in such way that the image representation we are looking for can cope with all variations of the features of interest and thus, is complete with respect to that concepts of structure descriptions. This includes another type of invariance, called relative invariance or equivariance. In the case of equivariance, a systematic change of input data will cause another systematic change of output data. For instance, it is known in signal processing that a shift of a function in input space will result in an equivalent phase change in Fourier domain.

#### 2.2.1 Invariance with Respect to Intrinsic Dimension

An image is locally composed by structures of different intrinsic dimension [50]. If the signal embedding dimension is two (a normal image signal), then a locally constant signal has intrinsic dimension zero (i0D), a non-bent edge or line has intrinsic dimension one (i1D), and all other bent structures including corners, junctions and end stopping points are of intrinsic dimension two (i2D). In figure 1 these types of intrinsic dimensions are demonstrated for some simple cases. From left to right follow a constant signal (i0D), an i1D signal which is always a rotated 1D signal and three different examples of i2D signals. The intrinsic dimension obviously corresponds to the number of degrees of freedom necessary to model a function. Responding to either edges/lines or corners/junctions makes a difference between detectors which are specific to intrinsic dimension. The eigenvalue analysis of the structure tensor is a well-known example. A special non-linear detector based on a Volterra series approach which is specific to i2D has been proposed in [29]. On the other hand, the monogenic signal [14], see also section 2.2, is specific to i1D structures. There is no detector available which responds to either i1D or i2D structure with a meaningful and rich set of features. It is well-known that the feature space spanned by mean and Gaussian curvature enables the classification with respect to intrinsic dimension [2], see also section 2.4. We will use that fact because we require completeness with respect to that concept.

**Fig. 1.** Example functions of different intrinsic dimension.

### 2.2.2 Invariance with Respect to Parity Symmetry

Parity symmetry locally indicates either symmetry or antisymmetry, respectively even or odd symmetry, of a structure in the case of reflection at a certain location. This enables e.g. classification as edge-like or line-like structure in i1D case and similarly in i2D case. Detectors should respond to both types of symmetry in the same manner but distinguishing. A counterexample is the structure tensor, which is sensible to edge-like structures because it is gradient based. Because the first order derivatives operator represents an odd function, it can only respond to odd structures in the sense of a matching operator. Because a second order derivative operator represents an even function, it responds to even structures. Hence, the combinations of both should deliver the required invariance. But this method has some drawbacks. Instead, most easily, parity symmetry can be decided from computing the local phase [42]. This can be achieved by so called quadrature filters. These detectors consist of two components which respond to either even or odd symmetry and which are in quadrature phase relation. That means, their components differ only by a phase shift of $\frac{\pi}{2}$. While this is an easy task for 1D signals, in 2D case this is not true. Nevertheless, the Gabor filter [19] is a popular candidate. Only in the framework of Clifford analysis certain concepts of multi-dimensional local phase can be reasonable formulated, because the topological situation can be modeled with sufficient degrees of freedom and with respect to the relations existing between these.

### 2.2.3 Invariance with Respect to Scale

Local image structure is restricted to a certain range of scale, called the intrinsic scale. Changing the scale will possibly change all other features. That is, intrinsic scale is a feature too [30] and a scale-adaptive scheme is advantageous in some cases. Traditionally, the Gaussian scale-space embedding of feature detection is used. Regrettably, the only feature which is intrinsic to a Gaussian scale-space is signal intensity. Only recently the monogenic scale-space has been proposed [16] as an alternative scale-space concept where local spectral representations, local orientation and other geometric features as angle of intersection become features of one single scale-space theory. This result from Clifford analysis will be adopted here.

### 2.2.4 Invariance with Respect to Rotation

Rotation invariance of detectors is an important requirement. Regrettably, the design of rotation invariant detectors is a non-trivial task. While the structure tensor and the Laplacian are rotation invariant, all detectors in the past based on quadrature filters in multiple dimensions were not [28]. The problem was that in the complex domain there could not be designed an isotropic odd filter which is in quadrature phase relation to its even counterpart. Only the Riesz transform as generalized Hilbert transform turned out to solve that problem in a Clifford valued domain [14]. This approach will also be used to formulate the harmonic conjugate part of the monogenic curvature tensor. Orientation is an important local feature of a structure which should be estimated in a rotation invariant way. In case of an i1D structure there are different methods available for orientation estimation, e.g. from the eigenvector analysis of the structure tensor respectively orientation tensor [3] or by using steerable filters [18]. These approaches do not give access to the other features mentioned in this section. Therefore, the monogenic signal is the method of choice because it delivers besides local energy and local phase also local orientation in a rotationally invariant manner. More complicated is the situation in the case of i2D structures which are related to multiple orientations meeting in a keypoint. Steerable filters can cope with that situation as well [34], while the structure tensor analysis delivers main and minor orientations which must not coincide with actual orientations of involved i1D structures. The same problems occur with the analysis of the monogenic curvature tensor. In [37], [21] and [36] different approaches for parametric modeling of corners have been proposed to cope with multiple orientations. Most interesting is the generalization of the structure tensor with respect to a multiple orientation model in [43].

### 2.2.5 Invariance with Respect to Angle of Intersection

Certain models of i2D structures as corners or junctions are described by superposition of i1D structures which meet in a keypoint. Hence, there are several geometric features describing such model. The most intuitive one besides orientation is the angle of intersection or apex angle. The detector of i2D structures should respond independent of the angle of intersection. The proposals in [36] and [43] are invariant with respect to the angle of intersection and rotationally invariant. In the framework of the monogenic signal a generalization has been proposed which is called structure multivector [15]. The involved model is two perpendicularly superimposed i1D structures. This rigid model has been generalized by the operator which delivers the monogenic curvature tensor. Another problem is estimating the angles of intersection in the case of multiple superimposed i1D structures. All mentioned methods need to know the number of superimposed patterns. For the assumption of two lines/edges with arbitrary but same phase and amplitude, we will present a phase based method in section 3 which results from the evaluation of the monogenic curvature tensor.

### 2.3 Monogenic Signal

In this section, we will give a short overview on the basic ideas of the monogenic signal as generalization of the analytic signal. More details can be found in the thesis [12] and in the papers [14, 42]. In the case of a real valued 1D signal $f : \mathbb{R} \to \mathbb{R}$ the extension to a complex valued signal $f_A : \mathbb{R} \to \mathbb{C}$, called analytic signal [19], is written in spatial domain as

$$f_A(x) = f(x) + j f_H(x) \; . \tag{1}$$

The components $f$ and $f_H$ are in quadrature phase relation, that is they are phase shifted by $\left|\frac{\pi}{2}\right|$. The imaginary completion $f_H$ is computed from the real signal $f$ by convolution with the Hilbert transform kernel

$$h(x) = \frac{1}{\pi x} \; . \tag{2}$$

Because the Hilbert transform is an all-pass operator, the use of quadrature filters $h_q$ in practice is preferred,

$$h_q(x) = h_e(x) + j h_o(x) \; . \tag{3}$$

This pair of even ($h_e$) and odd ($h_o$) operators is in quadrature phase relation within a chosen passband. The best known quadrature filter is the Gabor filter [19], which is also widely used in image processing, that is in case of 2D signals, as oriented quadrature filter [20]. Convolution of $f(\boldsymbol{x})$, $\boldsymbol{x} \in \mathbb{R}^n$, with $h_q(\boldsymbol{x})$ results in a separation of the output function, $g(\boldsymbol{x})$, with respect to symmetry,

$$g(\boldsymbol{x}) = g_e(\boldsymbol{x}) + j g_o(\boldsymbol{x}), \tag{4}$$

from which the local energy, $e(\boldsymbol{x})$, and the local phase, $\varphi(\boldsymbol{x})$, can be computed,

$$e(\boldsymbol{x}) = g_e^2(\boldsymbol{x}) + g_o^2(\boldsymbol{x}) \tag{5}$$

$$\varphi(\boldsymbol{x}) = \arg g(\boldsymbol{x}) \; . \tag{6}$$

But the lack of rotation invariance of the Gabor filter results in wrong estimates of $e$ and $\varphi$ in most cases. The need of a rotation invariant generalization of the Hilbert transform in multiple dimensions can be established within Clifford analysis [7]. We will assume that an $n$-dimensional function $f(\boldsymbol{x})$ is embedded into an $(n+1)$-dimensional space as vector field $\boldsymbol{f}(\boldsymbol{x}, x_{n+1}) = f(\boldsymbol{x})\boldsymbol{e}_{n+1}$ with $\boldsymbol{e}_i,\ i = 1, \ldots, n+1$ being unit vectors. Besides, we will assume a geometric algebra $\mathbb{R}_{n+1}$ over the vector space $\mathbb{R}^{n+1}$. Such geometric algebra is a linear space with a total number of $2^{n+1}$ well distinguishable subspaces of different grade. The unit subspace of highest grade is the so-called unit pseudoscalar $I_{n+1} = \boldsymbol{e}_1 \boldsymbol{e}_2 \cdots \boldsymbol{e}_{n+1}$. Then the Riesz transform kernel in either spatial or Fourier domain,

$$r_n(\boldsymbol{x}) = \frac{a_n \boldsymbol{x} \boldsymbol{e}_{n+1}}{|\boldsymbol{x}|^{n+1}} \quad \text{and} \quad R_n(\boldsymbol{u}) = \frac{\boldsymbol{u}}{|\boldsymbol{u}|} I_{n+1}^{-1} \tag{7}$$

results as solution of the Dirac equation for $x_{n+1} = 0$. It is an isotropic all-pass operator in any signal dimension $n$. Note that the geometric product of a geometric algebra is written by juxtaposition of the factors. Hence, in equation (7) the product $\boldsymbol{x}\boldsymbol{e}_{n+1}$ between the two vectors results in a bivector, belonging to another subspace as the original vectors. In addition, $a_n = \pi^{-\frac{n+1}{2}}\Gamma(\frac{n+1}{2})$ is a constant. If we restrict to the case $n = 2$, then the monogenic signal [14] as generalized analytic signal is represented by the vector field

$$\boldsymbol{f}_M(\boldsymbol{x}) = \boldsymbol{f}(\boldsymbol{x}) + \boldsymbol{f}^r(\boldsymbol{x}) = \boldsymbol{f}(\boldsymbol{x}) + (r_2 * \boldsymbol{f})(\boldsymbol{x}) \tag{8}$$

with $\boldsymbol{f}(\boldsymbol{x}) = f(\boldsymbol{x})\boldsymbol{e}_3$ and

$$\boldsymbol{f}^r(\boldsymbol{x}) = f^r_{(1)}(\boldsymbol{x})\boldsymbol{e}_1 + f^r_{(2)}(\boldsymbol{x})\boldsymbol{e}_2 \ . \tag{9}$$

As we see in equation (9), the convolution of the original vector field with the operator $r_2$ results in additional components which are laying in the image plane. A comparison with the analytic signal supports the interpretation that by the monogenic signal three orthogonal components are represented and that the complex domain is generalized in a certain way. In fact, it is useful to imagine a complex plane, the phase plane, oriented by the angle $\theta$ in $\mathbb{R}^3$ and spanned by the original signal $\boldsymbol{f}$ and the monogenic signal $\boldsymbol{f}_M$. According to equation (6), any phase angle indicates a certain local symmetry. The Riesz transform is a rotationally invariant and spinor valued operator which is identical with the first order circular harmonic. This operator rotates the original signal $\boldsymbol{f}(\boldsymbol{x}) = f(\boldsymbol{x})\boldsymbol{e}_3$ to $\boldsymbol{f}_M(\boldsymbol{x})$ by introducing the additional components $\boldsymbol{f}^r_{(1)}$ and $\boldsymbol{f}^r_{(2)}$. All three components constitute a Riesz triple, that is they are in quadrature phase. Figure 2 visualizes the effect of the Riesz transform.

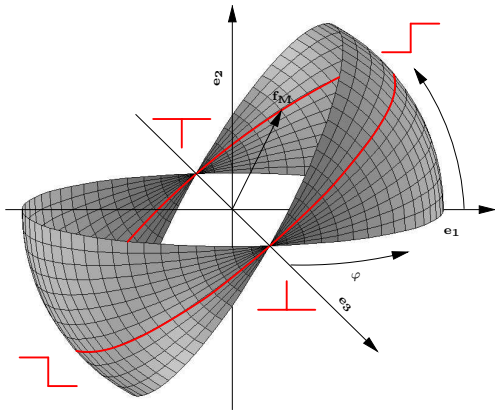


**Fig. 2.** The embedding of the monogenic signal in $\mathbb{R}^3$.

It delivers not only the right local spectral representations (in contrast to the Gabor filter) but in addition the orientation angle of the local struc-

ture. This is only half of the story because the complete solution of the Dirac equation for the open half space $x_{n+1} > 0$ gives rise to two additional transformations, represented by the scalar valued Poisson kernel

$$p(\boldsymbol{x};\sigma) = \frac{a_n \sigma}{|\boldsymbol{x} + \sigma \boldsymbol{e}_{n+1}|^{n+1}} \quad \text{and} \quad P(\boldsymbol{u};\sigma) = \exp(-2\pi|\boldsymbol{u}|\sigma) \tag{10}$$

and by the bivector valued conjugate Poisson kernel,

$$q(\boldsymbol{x};\sigma) = \frac{a_n \boldsymbol{x} \boldsymbol{e}_{n+1}}{|\boldsymbol{x} + \sigma e_{n+1}|^{n+1}} \quad \text{and} \quad Q(\boldsymbol{u};\sigma) = R_n(\boldsymbol{u}) P(\boldsymbol{u},\sigma) \tag{11}$$

with $|\boldsymbol{u}|$ being the absolute frequency value and $\sigma \equiv x_{n+1}$ being a scale parameter from which both kernels are parametrically depending on, as indicated by the semicolon in equations (10) and (11). Hence, $(\boldsymbol{x}, \sigma \boldsymbol{e}_{n+1})$ is spanning a linear and isotropic scale-space. The representation

$$\boldsymbol{f}_M(\boldsymbol{x},\sigma) = \boldsymbol{f}_p(\boldsymbol{x},\sigma) + \boldsymbol{f}_q(\boldsymbol{x},\sigma) \tag{12}$$

with

$$\boldsymbol{f}_p(\boldsymbol{x},\sigma) = (p(\sigma) * \boldsymbol{f})(\boldsymbol{x}) \tag{13}$$

and

$$\boldsymbol{f}_q(\boldsymbol{x},\sigma) = (q(\sigma) * \boldsymbol{f})(\boldsymbol{x}) \tag{14}$$

is the monogenic scale-space representation [16] of the original real valued signal $\boldsymbol{f}(\boldsymbol{x}) = f(\boldsymbol{x})\boldsymbol{e}_{n+1}$. As a consequence, the local spectral representations as well as the local orientation are getting scale-space representations too. Regrettably, the monogenic signal and the monogenic scale-space are only adequate multi-dimensional generalizations of the analytic signal with respect to i1D structures. Obviously, an enrichment of the used Clifford analysis framework with additional geometric modeling resources is needed. Therefore, we are adopting ideas from differential geometry and its tensor representations in a Clifford analysis framework as outlined in section 3.

### 2.4 Basics of Differential Geometry

Differential geometry is applied in image modeling since 1980th, pioneered by Koenderink and van Doorn [25], [24], and Besl and Jain [2]. An image is assumed to be a smooth surface $S$ embedded in $\mathbb{R}^3$ in an explicit parametric form with respect to a known coordinate system,

$$S(f) = \{(x,y,z) : x = d(u,v), y = e(u,v), z = f(u,v); (u,v) \in \mathbb{R}^2\}. \tag{15}$$

Besides the parametric representation this is similar to the vector field embedding used in Clifford analysis. Also smoothness is required in both approaches. For the sake of simplicity often a Monge patch representation [6] is used. This considerably simplifies the metric tensor $M(\boldsymbol{x})$ of the first fundamental form

and the curvature tensor $T(\boldsymbol{x})$ of the second fundamental form [2] for the scalar valued image function $f(\boldsymbol{x})$,

$$M(\boldsymbol{x}) = \begin{pmatrix} 1+f_x^2 & f_x f_y \\ f_x f_y & 1+f_y^2 \end{pmatrix}(\boldsymbol{x}), \quad T(\boldsymbol{x}) = (1+f_x^2+f_y^2)^{-\frac{1}{2}} B(\boldsymbol{x}) \tag{16}$$

with the Hessian matrix

$$B(\boldsymbol{x}) = \begin{pmatrix} f_{xx} & f_{xy} \\ f_{xy} & f_{yy} \end{pmatrix}(\boldsymbol{x}). \tag{17}$$

Although only up to second order derivatives are used, the associated tensor structure delivers rich insight with respect to local geometry. There are two curvature measures, the Gaussian curvature $\kappa(\boldsymbol{x})$ and the mean curvature $\mu(\boldsymbol{x})$ which are derived from the Weingarten mapping matrix $W(\boldsymbol{x}) = (M^{-1})T(\boldsymbol{x})$ according to

$$\kappa(\boldsymbol{x}) = \det(W)(\boldsymbol{x}) = \det(M^{-1})\det(T)(\boldsymbol{x}) \tag{18}$$

$$\mu(\boldsymbol{x}) = \frac{1}{2}\mathrm{trace}(W)(\boldsymbol{x}) = \frac{1}{2}\mathrm{trace}(M^{-1}T)(\boldsymbol{x}). \tag{19}$$

The determinant operator and the trace operator deliver the algebraic main invariants of second order tensors. In the Monge patch representation these curvature measures are written

$$\kappa(\boldsymbol{x}) = \frac{f_{xx}f_{yy} - f_{xy}^2}{(1+f_x^2+f_y^2)^2} \tag{20}$$

$$\mu(\boldsymbol{x}) = \frac{1}{2}\frac{f_{xx}(1+f_y^2) + f_{yy}(1+f_x^2) - 2f_{xy}f_x f_y}{(1+f_x^2+f_y^2)^{\frac{3}{2}}}. \tag{21}$$

### 2.5 Alternative Recent Tensor Representations

In recent years tensor representations became an attractive tool for different purposes of image analysis, for instance for the analysis of range images in a differential geometric framework [2] or for the representation of 3D surface orientations in the framework of quadrature filters [23]. In [44] the orientations of flow fields in image sequences are estimated. An overview on the use of tensors for analyzing orientated patterns is given in [3]. Finally, [33] present a linear tensor voting technique for salient feature inference. Regrettably, all these proposals are lacking the advantages resulting from a monogenic signal representation. In the following we will summarize some key features of recent tensor proposals with respect to the invariances mentioned in section 2.2. As we will show in section 3, all these invariances are fulfilled in the case of the monogenic curvature tensor. The structure tensor [17] delivers energy and orientation in a rotation invariant manner. But it responses only reasonable

to odd symmetric patterns. Thus, phase invariance is missed and no phase information is contained. The orientation tensor [4] can be also interpreted as a structure tensor, although a set of directed quadrature filters constitutes its elements. Nevertheless, it delivers no phase information. It is restricted to i1D structures but is phase invariant. The energy tensor [13], represents products of first and second order derivatives of a bandpass filtered image representation. Although it is invariant with respect to intrinsic dimension its phase invariance is restricted [27]. It represents no phase information. The gradient energy tensor [27] is composed by an even and an odd part. It delivers an energy measure which is invariant with respect to the intrinsic dimension but is not phase invariant. Most interestingly in our context is the boundary tensor [26]. As has been shown in [27], this tensor has the interesting property that its odd part is the Riesz transform of the even part. Nevertheless, although from that construction several invariances result (intrinsic dimension, phase, rotation), it represents an energy measure and thus fails to represent phase.

## 3 Monogenic Curvature Tensor and its Evaluation

In this section, we derive the monogenic curvature tensor by merging the concept of the monogenic signal with the Hessian matrix from differential geometry. We will evaluate the monogenic curvature tensor with respect to its determinant and trace. While the trace results in a representation of i1D signals, which is identical to the monogenic signal, the determinant delivers a novel signal representation for i2D signals. We will evaluate that signal representation with respect to local spectral representations and geometric features. This set of features will posses all invariance requirements formulated in section 2.2. Because the monogenic curvature tensor will be embedded in a monogenic scale-space, all derived features will get the same scale-space embedding.

### 3.1 Monogenic Curvature Tensor

Our approach of deriving the monogenic curvature tensor [48, 49] is based on lifting up a monogenic signal $\boldsymbol{f}_M \in \mathbb{R}_3$ into a tensor representation associated to the curvature tensor of differential geometry. Instead of taking the complete curvature tensor we restrict ourselves to the Hessian matrix, equation (17). We call the resulting tensor, $T(\boldsymbol{x}) : \mathbb{R}^2 \rightarrow M(2, \mathbb{R}_3)$, the monogenic curvature tensor although it is different from the curvature tensor in equation (16). The matrix geometric algebra $M(2, \mathbb{R}_3)$, see [39] is a much more powerful algebraic framework than the Euclidean geometric algebra $\mathbb{R}_3$ which is used in section 2.3. This can be concluded from the isomorphism $M(2, \mathbb{R}_{p,q}) \cong \mathbb{R}_{p+1,q+1}$ [31], hence, $M(2, \mathbb{R}_3) \cong \mathbb{R}_{4,1}$. The Hessian matrix with elements in $\mathbb{R}_3$, $B(\boldsymbol{x}) \in M(2, \mathbb{R}_3)$, applied to the original signal $\boldsymbol{f}(x)$ reads

$$B(\boldsymbol{x}) = \begin{pmatrix} f_{xx}\boldsymbol{e}_3 & -f_{xy}I_3 \\ f_{xy}I_3 & f_{yy}\boldsymbol{e}_3 \end{pmatrix} \tag{22}$$

with $I_3 = \boldsymbol{e}_1\boldsymbol{e}_2\boldsymbol{e}_3$ being the unit pseudoscalar of $\mathbb{R}_3$. This results from a tensorial convolution, $*_\tau$, of the signal $\boldsymbol{f}(\boldsymbol{x}) = f(\boldsymbol{x})\boldsymbol{e}_3$ with an even symmetric Hessian operator $\mathcal{H}_e \in M(2, \mathbb{R}_3^+)$, written as

$$h_e(\boldsymbol{x}) = \begin{pmatrix} \partial_{xx} & -\partial_{xy}\boldsymbol{e}_{12} \\ \partial_{xy}\boldsymbol{e}_{12} & \partial_{yy} \end{pmatrix} (\boldsymbol{x}), \tag{23}$$

and the definition of the first order derivative of the vector field $\boldsymbol{f}$, $\partial\boldsymbol{f}(\boldsymbol{x}) = \boldsymbol{e}_1\partial_x f(x,y)\boldsymbol{e}_3 + \boldsymbol{e}_2\partial_y f(x,y)\boldsymbol{e}_3 = f_x\boldsymbol{e}_{13} + f_y\boldsymbol{e}_{23}$. The minus sign in this equation results from the non-commutativity of the geometric product, hence, $\boldsymbol{e}_{21} = -\boldsymbol{e}_{12}$. Obviously, the elements of the Hessian operator are either scalars or bivectors. Both multivector types belong to the so-called even subalgebra of $\mathbb{R}_3$, which possesses only even-grade elements, as is indicated by $\mathbb{R}_3^+$. The term even symmetric as characterization of the Hessian operator follow from the fact that second order derivative operators are of even symmetry (in contrast to first order derivative operators which are of odd symmetry) and thus are responding to even-symmetric structures as lines. In case of odd symmetric structures their response would be zero. But we want to apply that operator on the monogenic signal $\boldsymbol{f}_M$ instead, and the result will be called the monogenic curvature tensor, $T_M$. Then it follows

$$T_M = \mathcal{H}_e\boldsymbol{f}_M = \mathcal{H}_e(\boldsymbol{f} + \boldsymbol{f}^r) = \mathcal{H}_e(\mathcal{I} + \mathcal{R})\boldsymbol{f} \tag{24}$$

with the identity operator $\mathcal{I}$ and the operator of the Riesz transform $\mathcal{R}$. According to equation (9), the function $\boldsymbol{f}^r$ indicates the monogenic completion of the function $\boldsymbol{f}$ resulting from the convolution of $\boldsymbol{f}$ with the Riesz kernel $r_2$, see equation (7). Because $\boldsymbol{f}_M \in C^\infty(\Omega)$ with $\Omega$ as an open region in $\mathbb{R}^2$, the partial derivatives of $\mathcal{H}_e$ will be applied without problems. In addition, supposed $\boldsymbol{f} \in L_2(\mathbb{R}^2, \mathbb{R}_3)$, then the commutativity $\mathcal{H}_e\mathcal{R} = \mathcal{R}\mathcal{H}_e$ will follow, see [9] for more details. So we can also formulate an odd Hessian operator $\mathcal{H}_o = \mathcal{R}\mathcal{H}_e$ and the monogenic curvature tensor will be composed by an even and an odd part,

$$T_M = (\mathcal{H}_e + \mathcal{H}_o)\boldsymbol{f} = T_e + T_o = T_e + \mathcal{R}T_e. \tag{25}$$

To get these relations more explicitly, we are going to the Fourier domain and express the operator $\mathcal{H}_e$ by polar coordinates $\boldsymbol{u} = (\varrho, \alpha)$. Then the even Hessian operator is separable,

$$H_e(\varrho, \alpha) = -\frac{4\pi^2\varrho^2}{2} \begin{pmatrix} 1 + \cos(2\alpha) & -\sin(2\alpha)\boldsymbol{e}_{12} \\ \sin(2\alpha)\boldsymbol{e}_{12} & 1 - \cos(2\alpha) \end{pmatrix}. \tag{26}$$

While the radial part $H_e(\varrho)$ expresses the well known highpass characteristics according to the derivative theorem of Fourier theory, the angular part

$H_e(\alpha)$ enables the investigation of local geometry. The angular part is written in terms of trigonometric functions according to the angular components of derivatives written in polar coordinates in spectral domain. These matrix entries can be related to the Fourier representation of circular harmonics of order $m \geqslant 0$,

$$C_m(\alpha) = \exp(m\alpha \boldsymbol{e}_{12}) = \cos(m\alpha) + \sin(m\alpha)\boldsymbol{e}_{12}. \tag{27}$$

Their radial part is constant, $C_m(\varrho) = \text{const}$. We want to express the Hessian operator in terms of regularized derivatives. This means to convert the highpass characteristic of $H_e(\varrho)$ to a bandpass characteristic. Because we are operating our signal analysis in a monogenic scale-space, the Poisson kernel, equation (10), can be used to define a difference of Poisson (DOP) kernel [16]

$$H_{DOP}(\varrho; \sigma_{BP}) = P(\varrho; \sigma_f) - P(\varrho; \sigma_c) \tag{28}$$

with $\sigma_f$ being a fine scale and $\sigma_c$ being a coarse scale so that $H_{DOP}$ will have its maximum at $\varrho_{BP} = \frac{1}{\sigma_{BP}}$. As a consequence, we are considering damped circular harmonic functions of order $m$ according to

$$C_m^P(\varrho, \alpha; \sigma) = H_{DOP}(\varrho; \sigma) C_m(\alpha)\ . \tag{29}$$

From this follows for the even Hessian operator $H_e(\varrho, \alpha; \sigma) = H_e(\varrho; \sigma) H_e(\alpha)$, represented in terms of circular harmonics as

$$H_e(\varrho, \alpha; \sigma) = \frac{1}{2} \begin{pmatrix} C_0^P + \langle C_2^P \rangle_0 & -\langle C_2^P \rangle_2 \\ \langle C_2^P \rangle_2 & C_0^P - \langle C_2^P \rangle_0 \end{pmatrix} (\varrho, \alpha; \sigma). \tag{30}$$

Here $\langle\ \ \rangle_0$ means the scalar part and $\langle\ \ \rangle_2$ means the bivector part of $C_2^P$. The odd Hessian operator follows simply as the Riesz kernel transformed even one and by remembering that the Riesz transform corresponds to a circular harmonic of first order. Hence,

$$H_o(\varrho, \alpha; \sigma) = (C_1^P \times_\tau H_e)(\varrho, \alpha; \sigma). \tag{31}$$

We are calling the operator $\mathcal{H}_M = \mathcal{H}_e + \mathcal{H}_o$ the monogenic Hessian operator, which applied to the original signal $\boldsymbol{f}$ results in the monogenic curvature tensor. What remains open is the discussion of its angular part $H_M(\alpha)$. As discussed in detail in [49, 48], it can be interpreted as a rotation invariant detector of i1D structures superimposed with arbitrary angles of intersection. This can be seen from re-writing the angular part of $H_e$ as

$$H_e(\alpha) = \begin{pmatrix} \cos^2(\alpha) & -\frac{1}{2}\sin(2\alpha)\boldsymbol{e}_{12} \\ \frac{1}{2}\sin(2\alpha)\boldsymbol{e}_{12} & \sin^2(\alpha) \end{pmatrix}\ . \tag{32}$$

The two functions on the diagonal and that one on the anti-diagonal, $\sin(2\alpha) = \cos^2(\alpha - \frac{\pi}{4}) - \sin^2(\alpha - \frac{\pi}{4})$, constitute four basis functions to steer a detector for even symmetric i1D structures. In figure 3 their effect on the pattern to the left is shown. The same arguments lead to the interpretation of the entries of $H_o(\alpha)$ as rotationally invariant detector of odd symmetric i1D structures.

From this interpretation of the monogenic Hessian operator follows that it analyzes i2D structures as superposition of i1D structures.

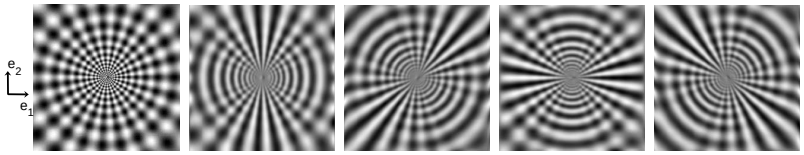


**Fig. 3.** Action of the even angular windowing functions on the left most test image.

### 3.2 Evaluation of the Monogenic Curvature Tensor

In this section, we give a short sketch on the ways the structural information of the monogenic curvature tensor can be evaluated. More details can be found in [48]. As a result of the preceding section we can state the invariance of this representation with respect to scale, parity symmetry and rotation. Here we will show the invariance with respect to intrinsic dimension and the derivation of local spectral features as well as geometric features.

#### 3.2.1 Local Representations for i1D and i2D Structures

As is known from real valued differential geometry [2], structures of different intrinsic dimension can be classified in a space spanned by Gaussian curvature, $\kappa$, and mean curvature, $\mu$. Both are computed from the curvature tensor by applying either the determinant or the trace operator. If we are doing the same in our algebraic framework $M(2,\mathbb{R}_3)$, we get two different signal representations which are specific to the intrinsic dimension. The first one is a vector field specific to i1D structures,

$$\boldsymbol{f}_{i1D}(\boldsymbol{x}) = \boldsymbol{t}_e(\boldsymbol{x}) + \boldsymbol{t}_o(\boldsymbol{x}) = \mathrm{trace}(T_e)(\boldsymbol{x}) + \mathrm{trace}(T_o)\boldsymbol{e}_2(\boldsymbol{x}) \tag{33}$$

$$= \boldsymbol{f}(\boldsymbol{x}) + (c_1 * \boldsymbol{f})(\boldsymbol{x}) \equiv \boldsymbol{f}_M(\boldsymbol{x}). \tag{34}$$

That is, the trace operation reconstructs the monogenic signal from the monogenic curvature tensor. Here $c_1$ is the first order circular harmonic, which is identical to the Riesz transform. By computing the determinant of $T(\boldsymbol{x})$ another vector field specific to i2D structures will result.

$$\boldsymbol{f}_{i2D}(\boldsymbol{x}) = \boldsymbol{d}_e(\boldsymbol{x}) + \boldsymbol{d}_o(\boldsymbol{x}) = \det(T_e)\boldsymbol{e}_3(\boldsymbol{x}) + \boldsymbol{e}_1\det(T_o)(\boldsymbol{x}) \tag{35}$$

$$= \boldsymbol{d}_e(\boldsymbol{x}) + (\boldsymbol{e}_1 c_2 \boldsymbol{e}_3 * \boldsymbol{d}_e)(\boldsymbol{x}) \equiv \boldsymbol{f}_{MC}(\boldsymbol{x}). \tag{36}$$

Note that the computation of the determinant in the algebraic framework $M(2,\mathbb{R}_3)$ is in general rather expensive, see [39]. But a thorough analysis of our case [48] did yield the same computation as in $M(2,\mathbb{R})$. This signal representation is called "generalized monogenic" curvature signal because its conjugate harmonic part results from the real part by applying a second order circular harmonic as another generalized Hilbert transform [8]. While the structure of both signal representations is the same, they are coding quite different properties of a local signal structure. They enable classification with respect to the intrinsic dimension.

### 3.2.2 Local Spectral Representations

Both signal representations can be interpreted as the result of a spinor valued operator, $\mathcal{S}$, which rotates and scales the original vector field $\boldsymbol{f}(\boldsymbol{x}) = f(x,y)\boldsymbol{e}_3$ so that it will be supplemented by a conjugate harmonic component which projects to the plane $\boldsymbol{e}_1 \wedge \boldsymbol{e}_2$ and fulfills the conditions $\boldsymbol{t}_e^2 = \boldsymbol{t}_o^2$ and $\boldsymbol{d}_e^2 = \boldsymbol{d}_o^2$. The scaling-rotation is performed in the 'phase plane' expressed by the outer product $\boldsymbol{f}_s(\boldsymbol{x}) \wedge \boldsymbol{e}_3 = \langle \boldsymbol{e}_3 \boldsymbol{f}_s(\boldsymbol{x})\rangle_2$ with $s(\boldsymbol{x}) = \boldsymbol{e}_3\boldsymbol{f}_s(\boldsymbol{x})$ being the respective spinor and $\boldsymbol{f}_s \equiv \boldsymbol{f}_{i1D}$ or $\boldsymbol{f}_s \equiv \boldsymbol{f}_{i2D}$. That is, for both $\boldsymbol{f}_{i1D}$ and $\boldsymbol{f}_{i2D}$ a similar model for the monogenic extension of the real valued function $\boldsymbol{f}$ is assumed. Only the involved generalized Hilbert transform differs. Therefore, also the computation of the local features in both cases is the same. By evaluating the exponential representation of $s$ with respect to the $\mathbb{R}_3^+$-logarithm, see [12] and [42] for more details, the local spectral representations can be computed. These are the local amplitude

$$a(\boldsymbol{x}) = |\boldsymbol{f}_s(\boldsymbol{x})| = \exp(\langle \log(\boldsymbol{e}_3\boldsymbol{f}_s(\boldsymbol{x}))\rangle_0) \tag{37}$$

and the (generalized) monogenic local phase bivector

$$\Phi(\boldsymbol{x}) = \arg(\boldsymbol{f}_s(\boldsymbol{x})) = \langle \log(\boldsymbol{e}_3\boldsymbol{f}_s(\boldsymbol{x}))\rangle_2. \tag{38}$$

From $\Phi(\boldsymbol{x})$ follow the local phase $\varphi(\boldsymbol{x})$ as rotation angle within the phase plane,

$$\varphi(\boldsymbol{x}) = |(\Phi(\boldsymbol{x}))^\star| = \arctan\left(\frac{|\langle \boldsymbol{e}_3\boldsymbol{f}_s(\boldsymbol{x})\rangle_2|}{|\langle \boldsymbol{e}_3\boldsymbol{f}_s(\boldsymbol{x})\rangle_0|}\right), \tag{39}$$

and the orientation angle of the phase plane

$$\theta(\boldsymbol{x}) = \frac{\langle \boldsymbol{e}_3\boldsymbol{f}_s(\boldsymbol{x})\rangle_2}{|\langle \boldsymbol{e}_3\boldsymbol{f}_s(\boldsymbol{x})\rangle_2|}\,. \tag{40}$$

Here the star in equation (39) indicates the duality operation which converts the local phase bivector $\Phi(\boldsymbol{x})$ into the local rotation vector $(\Phi(\boldsymbol{x}))^\star$, the magnitude of which is the local phase $\varphi(\boldsymbol{x})$. The interpretation of the local spectral representations and of the local orientation derived from the monogenic signal is well known for i1D structures. I2D structures will be also seen from the monogenic signal as i1D structures. Hence, it delivers mean orientation for any phases of the contributing i1D structures and mean phase only in case of equal phases of the contributing i1D structures. But this is no serious restriction in reality. The interpretation of the features derived from the generalized monogenic curvature signal is not so obvious. As has been discussed in section 3.1, a first hint results from the interpretation of the monogenic Hessian operator in Fourier domain. That is, i2D patterns are seen by the operator as superposition of i1D patterns and each of them contributes to the monogenic curvature tensor representation. Hence, the i1D-view on the structure as known from the monogenic signal is not left in case of the monogenic curvature tensor representation. But a more detailed analysis of this

fact in Fourier domain has not been done. Instead, a careful analysis of the monogenic curvature tensor in the Radon domain [47] has been performed. The results confirm that the monogenic curvature tensor in the case of superimposed i1D structures delivers mean phase and mean orientation, just as the monogenic signal itself. Therefore, the proposed signal representation seems to be not a sufficient extension for the extraction of local spectral features of i2D structures. Nevertheless, several applications confirm the usefulness of the proposed signal representation, e.g. as corner detector or as phase based constraint in image sequence analysis. It can be shown that the determinant of the even part of the monogenic curvature tensor equals zero iff the underlying signal structure is of intrinsic dimension one. These results are illustrated in figure 4 and can be used as a rotational invariant corner detector.
For further results the reader is advised to have a look on our website `http://www.ks.informatik.uni-kiel.de/`.


**Fig. 4.** Original image and local information by the determinant of the even part of the monogenic curvature tensor. One representative i2D corner is marked by the red rectangle.

### 3.2.3 The Angle of Intersection

The monogenic curvature tensor enables to compute the angle of intersection or apex angle of two superimposed i1D signals. To calculate the angle of intersection or apex angle $\alpha \in \left[0, \frac{\pi}{2}\right]$ of two superimposed i1D signals where each one of them can have arbitrary phase in terms of the monogenic signal the following trick is to consider the resulting image structure as one locally intrinsic i2D hyperbolic saddle point model with *absolute* main curvature values. This model is completely described by its two main curvatures $\kappa_1$ and $\kappa_2$ which are related to the Gaussian curvature $\kappa = \kappa_1\kappa_2$ and the mean curvature $\mu = \frac{1}{2}(\kappa_1 + \kappa_2)$. The two main curvatures lie on the two orthogonal bisectors of the superimposed i1D signals. Only in direction of the two i1D signals the curvature $\kappa\left(\frac{\alpha}{2}\right)$ of the normal cut is zero. Now the surface theoretical results of Euler's and Meusnier's theorems [5]

$$\kappa\left(\frac{\alpha}{2}\right) = \lim_{\nu \to 0} \kappa_1 \cos^2\frac{\alpha}{2} + 2\nu \sin\frac{\alpha}{2}\cos\frac{\alpha}{2} + \kappa_2 \sin^2\frac{\alpha}{2} \tag{41}$$

can be used to determine the apex angle of our assumed model

$$\kappa\left(\frac{\alpha}{2}\right) = 0 \Rightarrow \alpha = 2\tan^{-1}\sqrt{\frac{|\kappa_1|}{|\kappa_2|}}, \tag{42}$$

where $\frac{\alpha}{2}$ is the angle relatively to the orientation with main curvature $\kappa_1$. Merging i1D signal theory and differential geometry delivers the exact apex angle

$$\alpha = 2\tan^{-1}\frac{|\varphi_1'|}{|\varphi_2'|}. \tag{43}$$

Here $\varphi_i'$ is the i1D phase change at the point of interest in direction of the main curvatures $\kappa_i$ $\forall i \in \{1, 2\}$ which have the same orientation as the two orthogonal main orientations of the i2D image structure. Applying this result to the monogenic curvature tensor in scale-space the apex angle can be computed by

$$\alpha(\boldsymbol{x}) = 2\tan^{-1}\sqrt{\left|\frac{\boldsymbol{t}_e(\boldsymbol{x}) - \sqrt{\boldsymbol{t}_e^2(\boldsymbol{x}) - \boldsymbol{d}_e(\boldsymbol{x})}}{\boldsymbol{t}_e(\boldsymbol{x}) + \sqrt{\boldsymbol{t}_e^2(\boldsymbol{x}) - \boldsymbol{d}_e(\boldsymbol{x})}}\right|}. \tag{44}$$

Each i2D corner can be locally modeled by two superimposed i1D structures in scale space. The computation of the angle of intersection is illustrated in figure 5 for each test point within the image. At points of intrinsic dimension one the angle of intersection modulo 180 degrees is zero. Therefore, the intrinsic dimension can be naturally determined by the angle of intersection. Note, that in figure 5 inner and outer corners can be also separated and detected by our approach in a rotational invariant way.


**Fig. 5.** Original image and local angle of intersection information. The monogenic curvature tensor is able to differ between inner and outer corners. The black corner with intersection angle of 270° is marked by the red rectangle and the white corner with intersection angle of 90° is marked by the blue rectangle.

## 4 Conclusions

This chapter presents a novel approach for local analysis of images. The proposed monogenic curvature tensor results from combining differential geometry and Clifford analysis in the setting of image analysis. The monogenic extension of a two-dimensional signal is lifted up to a new generalization of the analytic signal in a non-linear way. The generalized monogenic curvature signal can be evaluated just in the same way as the monogenic signal. But as has been shown in other work, the extracted features do no leave the i1D view on the signal. Therefore, future studies are required to cope with i2D structures and to derive meaningful local features. One way could be to include the Weingarten mapping in the signal representation. Another way could be the extension of the Radon transform for curved lines and to generalize the monogenic signal in that way. We followed that way and recently we proposed a conformal monogenic signal [46], [45], in which lines as i1D structures and circles as i2D structures are handled in the same framework.

## References

1. H. Bay, T. Tuytelaars, and L. Van Gool. SURF: Speed up robust features. In A. Leonardis, M. Bischof, and A. Pinz, editors, *ECCV*, volume 3951 of *LNCS*, pages 404–417. Springer-Verlag, Berlin, Heidelberg, New York, 2006.
2. P. J. Besl and R. C. Jain. Invariant surface characteristics for 3D object recognition in range images. *Comput. Vision Graph. Image Process.*, 33(1):33–80, 1986.
3. J. Bigün. *Vision with Direction*. Springer-Verlag, Berlin, Heidelberg, New York, 2006.
4. J. Bigün and G. H. Granlund. Optimal detection of linear symmetry. In *Proc. IEEE First Int. Conf. on Computer Vision*, pages 433–438, 1984.
5. W. Blaschke and K. Leichtweiß. *Elementare Differentialgeometrie*. Springer-Verlag, Berlin, Heidelberg, New York, 1973.
6. E. D. Bloch. *A First Course in Geometric Topology and Differential Geometry*. Birkhäuser, Boston, 1997.
7. F. Brackx, R. Delanghe, and F. Sommen. *Clifford Analysis*. Pittman, Boston, 1982.
8. F. Brackx, B. De Knock, and H. De Schepper. Generalized multidimensional Hilbert transforms in Clifford analysis. *International Journal of Mathematics and Mathematical Sciences*, 2006.
9. F. Brackx and H. De Schepper. Hilbert-Dirac operators in Clifford analysis. *Chin. Ann. Math.*, 26(1):1–14, 2005.
10. D.A. Danielson. *Vectors and Tensors in Engineering and Physics*. Addison-Wesley Publ. Company, Redwood City, 1992.
11. C.T.J. Dodson and T. Poston. *Tensor Geometry*. Springer-Verlag, Berlin, Heidelberg, New York, 1997.
12. M. Felsberg. *Low-Level Image Processing with the Structure Multivector*. PhD thesis, Technical Report No. 2016, Christian-Albrechts-Universität zu Kiel, Institut für Informatik und Praktische Mathematik, 2002.

13. M. Felsberg and G. H. Granlund. POI detection using channel clustering and the 2D energy tensor. In *Pattern Recognition*, volume 3175 of *LNCS*, pages 103–110. Springer-Verlag Berlin, Heidelberg, New York, 2004.
14. M. Felsberg and G. Sommer. The monogenic signal. *IEEE Transactions on Signal Processing*, 49(12):3136–3144, 2001.
15. M. Felsberg and G. Sommer. The structure multivector. In L. Dorst, C. Doran, and J. Lasenby, editors, *Applications of Geometric Algebra in Computer Science and Engineering*, pages 437–448. Birkhäuser, Boston, 2002.
16. M. Felsberg and G. Sommer. The monogenic scale-space: A unifying approach to phase-based image processing in scale-space. *Journal of Mathematical Imaging and Vision*, 21:5–26, 2004.
17. W. Förstner and E. Gülch. A fast operator for detection and precise location of distinct points, corners and centres of circular features. In *Proc. ISPRS Intercommission Workshop*, pages 149–155, Interlaken, 1987.
18. W. T. Freeman and E. H. Adelson. The design and use of steerable filters. *IEEE Trans. on Pattern Analysis and Machine Intelligence*, 13(9):891–906, 1991.
19. D. Gabor. Theory of communication. *Journal IEE*, 93(26):429–457, 1946.
20. G. H. Granlund and H. Knutsson. *Signal Processing for Computer Vision*. Kluwer Academic Publishers, Dordrecht, 1995.
21. A. Guiducci. Corner characterization by differential geometry techniques. *Pattern Recognition Letters*, 8:311–318, 1988.
22. D. Hestense and G. Sobczyk. *Clifford Algebra to Geometric Calculus*. Reidel, Dordrecht, 1984.
23. H. Knutsson. Representing local structure using tensors. In *Proc. of 6th Scandinavian Conference on Image Analysis*, pages 244–251, 1989.
24. J. J. Koenderink. The structure of images. *Biol. Cybernetics*, 50:363–370, 1984.
25. J. J. Koenderink and A. J. van Doorn. The structure of two-dimensional scalar fields with applications to vision. *Biol. Cybernetics*, 33:151–158, 1979.
26. U. Köthe. Integrated edge and junction detection with the boundary tensor. In *Proceeding of 9th Intl. Conf. on Computer Vision*, volume 1, pages 424–431, 2003.
27. U. Köthe and M. Felsberg. Riesz transform vs. derivatives: On the relationship between the boundary tensor and the energy tensor. In R. Kimmel, N. Sochen, and J. Weickert, editors, *Scale Space and PDE Methods in Computer Vision*, volume 3459 of *LNCS*, pages 179–191. Springer-Verlag, Berlin, Heidelberg, New York, 2005.
28. P. Kovesi. *Invariant Measures of Image Features from Phase Information*. PhD thesis, PhD thesis, University of Western Australia, Institute of Computer Science, Perth, 1996.
29. G. Krieger and C. Zetzsche. Nonlinear image operators for the evaluation of local intrinsic dimensionality. *IEEE Trans. on Image Processing*, 5(6):1026–1042, 1996.
30. T. Lindeberg. Feature detection with automatic scale selection. *Internat. Journal of Computer Vision*, 30(2):79–116, 1998.
31. P. Lounesto. *Clifford Algebras and Spinors*. London Mathematical Society Lecture Note Series. Cambridge University Press, 1997.
32. D. Lowe. Distinctive image features from scale-invariant keypoints, cascade filtering approach. *Int. Journal of Computer Vision*, 60:91–110, 2004.
33. G. Medioni, M. S. Lee, and C. K. Tang. *A Computational Framework for Segmentation and Grouping*. Elsevier, 2000.

34. M. Michaelis and G. Sommer. Junction classification by multiple orientation detection. In *ECCV*, volume 801 of *LNCS*, pages 101–108. Springer-Verlag, Berlin, Heidelberg, New York, 1994.
35. K. Mikolajczyk and C. Schmid. A performance evaluation of local descriptors. *IEEE Trans. Pattern Analysis and Maschine Intell.*, 27:1615–1630, 2005.
36. K. Rangarajan, M. Shah, and D. Van Brackle. Optimal corner detector. *Computer Vision, Graphics and Image Processing*, 48:230–245, 1989.
37. K. Rohr. Recognizing corners by fitting parametric models. *Int. Journal of Computer Vision*, 9(3):213–230, 1992.
38. K. Rohr. Localization properties of direct corner detectors. *Journ. Math. Imaging and Vision*, 4:133–150, 1994.
39. G. Sobczyk and G. Erlebacher. Hybrid matrix geometric algebra. In H. Li, P. J. Olver, and G. Sommer, editors, *Computer Algebra and Geometric Algebra with Applications*, volume 3519 of *LNCS*, pages 191–206. Springer-Verlag, Berlin, Heidelberg, New York, 2005.
40. G. Sommer. *Geometric Computing with Clifford Algebras*. Springer-Verlag, Berlin, Heidelberg, New York, 2001.
41. G. Sommer and C. Gebken. Robot vision in the language of geometric algebra. In G. Obinata and A. Dutta, editors, *Vision Systems: Applications*, pages 459–486. I-Tech Education and Publishing, Vienna, 2007.
42. G. Sommer and D. Zang. Parity symmetry in multi-dimensional signals. *Communications in Pure and Applied Analysis*, 6(3):829–852, 2007.
43. I. Stuke, T. Aach, E. Barth, and C. Mota. Analysing superimposed oriented patterns. In *6th IEEE Southwest Symposium on Image Analysis and Interpretation, Lake Tahoe, NV*, pages 133–137, 2004.
44. C. F. Westin. *A Tensor Framework for Multidimensional Signal Processing*. PhD thesis, Linköping University, Sweden, SE-581 83 Linköping, Sweden, 1994. Dissertation No 348, ISBN 91-7871-421-4.
45. L. Wietzke, O. Fleischmann, and G. Sommer. 2D image analysis by generalized Hilbert transforms in conformal space. In *ECCV*, LNCS. Springer-Verlag, Berlin, Heidelberg, New York, 2008. accepted.
46. L. Wietzke and G. Sommer. The conformal monogenic signal. In G. Rigoll, editor, *Pattern Recognition*, volume 5096 of *LNCS*, pages 527–536. Springer-Verlag, Berlin, Heidelberg, New York, 2008.
47. L. Wietzke, G. Sommer, C. Schmaltz, and J. Weickert. Differential geometry of monogenic signal representations. In G. Sommer and R. Klette, editors, *Robot Vision*, volume 4931 of *LNCS*, pages 454–465. Springer-Verlag, Berlin, Heidelberg, New York, 2008.
48. D. Zang. *Signal Modeling for Two-dimensional Image Structures and Scale-Space Based Image Analysis*. PhD thesis, Christian-Albrechts Universität zu Kiel, 2007. Technical Report No. 0705.
49. D. Zang and G. Sommer. Signal modeling for two-dimensional image structures. *Journal of Visual Communication and Image Representation*, 18(1):81–99, 2007.
50. C. Zetzsche and E. Barth. Fundamental limits of linear filters in the visual processing of two-dimensional signals. *Vision Research*, 30:1111–1117, 1990.